Int. J. Electrochem. Sci., 10 **(2015)** 9351 - 9358

International Journal of
ELECTROCHEMICAL
SCIENCE
www.electrochemsci.org

Short Communication

Effect of Temperature on the Electrochemical Performance of $LiCu_{0.04}Mn_{1.96}O_4$ Prepared by a Molten-Salt Combustion Method

Wangqiong Xu[1,2], *Jijun Huang*[1,2], *Qiling Li*[1,2], *Hongli Bai*[1,2], *Changwei Su*[1,2], *Yonghui He*[1,2], *Wei Bai*[1,2], *Junming Guo*[1,2,*]

[1] Key Laboratory of Resource Clean Conversion in Ethnic Regions，Education Department of Yunnan, Yunnan Minzu University, Kunming 650500, PR China
[2] Joint Research Centre for International Cross-border Ethnic Regions Biomass Clean Utilization in Yunnan, Yunnan Minzu University, Kunming 650500, PR China
[*]E-mail: guojunming@tsinghua.org.cn

Received: 28 July 2015 / *Accepted:* 15 September 2015 / *Published:* 30 September 2015

Spinel $LiCu_{0.04}Mn_{1.96}O_4$ compounds were fabricated by a molten-salt combustion method. The results of X-ray diffraction (XRD) analysis and scanning electron microscopy (SEM) confirm that the copper additive incorporates into the $LiMn_2O_4$ lattice, the lattice parameters and average particle size increase gradually with increasing two-stage calcination temperatures. The effect of two-stage calcination temperature on the electrochemical properties of the $LiCu_{0.04}Mn_{1.96}O_4$ materials was investigated by galvanostatic charge/discharge tests and cyclic voltammetry (CV). Results showed that the structural stability of the materials was improved due to Cu-doping. The $LiCu_{0.04}Mn_{1.96}O_4$ materials calcined at 600 ℃ demonstrated excellent electrochemical performance with an initial discharge specific capacity of 119.1 mAh g^{-1}, and the capacity retention was 90.6% after 100 cycles at 0.5 C.

Keywords: Lithium-ion battery; molten-salt combustion method; Cu doping; $LiMn_2O_4$

1. INTRODUCTION

Spinel $LiMn_2O_4$ has attracted a great deal of attention as the most promising positive-electrode material for lithium-ion battery pertaining to its advantages such as low cost, high safety , nontoxicity and environmental friendliness[1-2]. However, the rapid capacity fading of $LiMn_2O_4$ currently restricts its practical use. The rapid capacity fading is mainly caused by structural distortion resulting from the Jahn-Teller effect[3]. Ion doping with cations like Zn^{2+} [4], Al^{3+} [5],Ce^{4+}[6] and Ni^{2+} [7] is an effective

way to improve the structural stability and electrochemical performance of $LiMn_2O_4$ as a cathode material. Doping $LiMn_2O_4$ with Cu can improve its structural stability because Cu-O bonds are stronger than Mn-O ones, which can improve the structural stability[8].

The process used to synthesis spinel $LiMn_2O_4$ is another important factor that affects its electrochemical performance as a cathode material. $LiMn_2O_4$ has been prepared by solid-state [9], co-precipitation route [10], sol-gel [11],polymer-pyrolysis method[12] and combustion methods [13]. sol-gel method gets more researched in present synthesis routs. Electrochemical performance of cathode materials is improved by this method, but sol-gel method were difficult to achieve large-scale industrial production because of synthesis technology is complicated, experiment conditions are harshing, chelating agents and fuels are added to raw materials. Spinel $LiMn_2O_4$ was firstly synthesized by the traditional solid-state process, which was simple and easy to achieve industrial production. But during the synthesis, high temperature and long reaction time were required and synthetic products agglomerated seriously, which led to poor electrochemical performance for $LiMn_2O_4$ materials [14].

In our previous works, the effect of Cu^{2+} and Mg^{2+} doped on electrochemical performance of the $LiMn_2O_4$ cathode materials prepared by molten-salt combustion synthesis[15,16]. However, the previous works were focus on the amount of Cu^{2+} and Mg^{2+} doped on electrochemical performance of the $LiMn_2O_4$ powders. In this works, we emphasized on researching effect two-stage calcination temperatures on electrochemical performance of the $LiCu_{0.04}Mn_{1.96}O_4$ cathode materials. Crystal structure, morphology and electrochemical properties of the $LiCu_{0.04}Mn_{1.96}O_4$ cathode materials were investigated in detail.

2. EXPERIMENT

2.1. Preparation of samples

Spinel $LiCu_{0.04}Mn_{1.96}O_4$ samples were synthesized by a molten-salt combustion method. At first, $CH_3COOLi{\cdot}2H_2O$, $Mn(CH_3COO)_2{\cdot}4H_2O$, $Cu(CH_3COO)_2{\cdot}H_2O$ with a stoichiometric molar ratio of 1:1.96:0.04 were weighed and placed in a 300 ml ceramic crucible. Then, the mixture was heated in a muffle furnace at 400 °C for 1h to get the precursor. The precursor was ground and calcined at 500 °C, 600 °C, 700 °C and 800 °C for 3h in a muffle furnace and then free cooling down to room temperature yielding the $LiCu_{0.04}Mn_{1.96}O_4$ powders finally(samples were marked II500, II600, II700 and II800, respectively).

2.2. Characterization

The crystalline structure of the product was analyzed using X-ray diffraction (XRD; D/max-TTRIII, Rigaku, Japan) with Cu Kα radiation in the 2θ angular range of 10–70° with a step size of 0.02° and scan speed of 4° min^{-1} at an operating current of 30 mA and voltage of 40 kV. Lattice

parameters were obtained using Jade 5.0 software. The morphology of the $LiCu_{0.04}Mn_{1.96}O_4$ powders was observed on the scanning electron microscopy (SEM; Quanta-200, FEI, Hillsboro, OR, USA).

2.3. Electrochemical measurements

The $LiCu_{0.04}Mn_{1.96}O_4$ electrode was prepared by mixing the $LiCu_{0.04}Mn_{1.96}O_4$ powder, carbon black and polyvinylidene fluoride(PVDF) with a mass ratio of 80:10:10. Then, N-methyl-2-pyrrolidon(NMP) was added to the mixture forming a homogeneous slurry. The slurry was pasted onto an Al foil current collector and dried at 120 °C under vacuum oven for overnight. The cathodes were punched into disks with a diameter of 16 mm. For electrochemical measurements, CR2025 coin-type cells were assembled in an argon-filled glove box using an $LiCu_{0.04}Mn_{1.96}O_4$ cathode, Li foil anode, polypropylene microporous film (Celgard 2320) separator, and electrolyte of 1.0 M $LiPF_6$ dissolved in ethylene carbonate and dimethyl carbonate (1:1 in volume). Galvanostatic charge and discharge tests of the cells were performed using a Land electric test system (CT2001A, Wuhan Jinnuo Electronics Co., Ltd., China) at a current density of 0.5 C (1 C=148mA g^{-1})in the potential range between 3.0 and 4.5 V. Cyclic voltammetry (CV) was conducted on an electrochemical workstation (IM6ex, Zahner Elektrik GmbH&Co. KG, Germany) in the voltage range of 3.5-4.6 V at a scanning rate of 0.05 mV s^{-1}.

3. RESULTS AND DISCUSSION

3.1 X-ray diffraction analysis

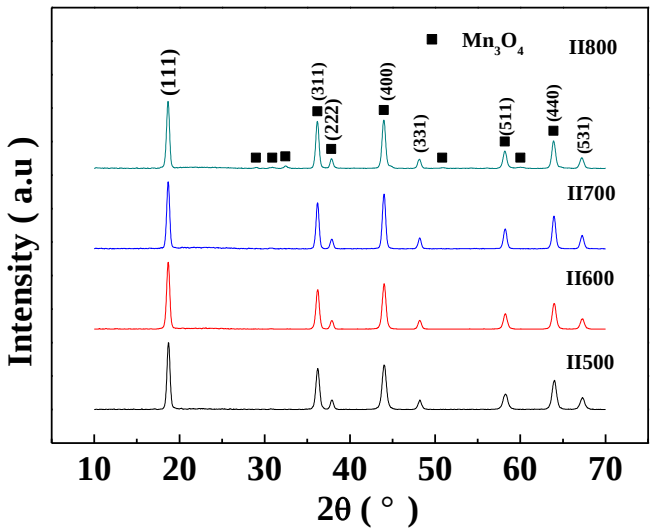

Figure 1. XRD patterns of the $LiCu_{0.04}Mn_{1.96}O_4$ materials prepared at calcination temperatures from II500 to II800.

Fig. 1 shows the XRD patterns of $LiCu_{0.04}Mn_{1.96}O_4$ powders prepared by the molten-salt combustion method at 400 ℃ for 1 h and two-stage calcination at 500 ℃, 600 ℃, 700 ℃ and 800 ℃ for 3 h, respectively. All $LiCu_{0.04}Mn_{1.96}O_4$ samples are in agreement with the standard pattern of spinel $LiMn_2O_4$. There is no marked difference in the crystal structure after calcinating at different temperatures. The results suggested that the major spinel structure of $LiMn_2O_4$ was not seriously changed after the two-stage calcination process. The XRD patterns of II500, II600 and II700 are consistent with a single phase, while a small amount of an impurity phase is detected in the pattern of II800, and can be identified as Mn_3O_4. The lattice parameters of the materials are summarized in Table 1.

Table 1. Lattice parameter of all samples.

Cathode material	Lattice parameter (Å)
II500	8.2249
II600	8.2308
II700	8.2316
II800	8.2377

Lattice parameters increase with the increase of calcination temperature, which indicates that the enhancement of reaction temperature is beneficial for the expansion of unit cell [17, 18]. What's more, the lattice parameters of all samples were less than the standard value 8.247Å of spinel $LiMn_2O_4$ [19], which indicated that Cu^{2+} ions were incorporated into the spinel $LiMn_2O_4$ lattice.

3.2 Morphology and particle size analysis

Fig. 2 presents the SEM images of $LiCu_{0.04}Mn_{1.96}O_4$ powders prepared by one-stage calcination at 400 ℃ for 1 h and two-stage calcination at 500 ℃, 600 ℃, 700 ℃ and 800 ℃ for 3h, respectively. As we can seen that the size distribution ranges of II500 and II600 products are from 110 to 171 nm, the size distribution ranges of II700 product is from 285 to 860 nm.

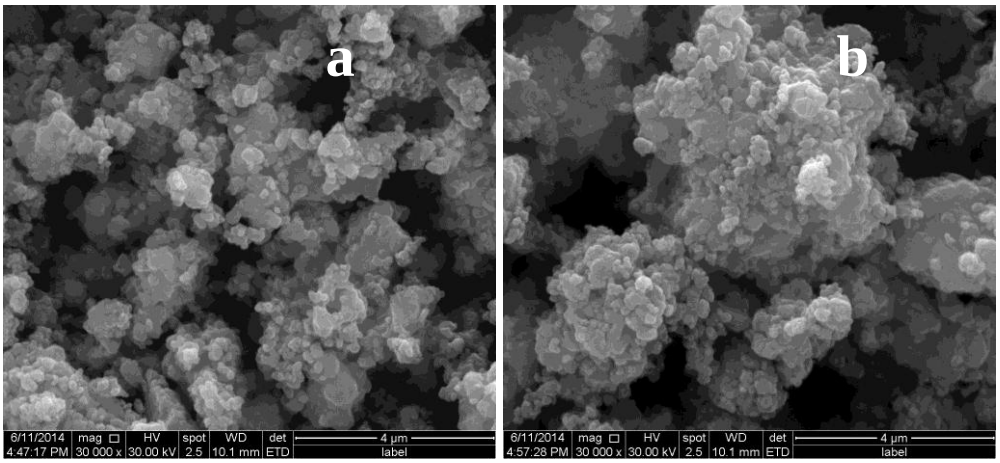

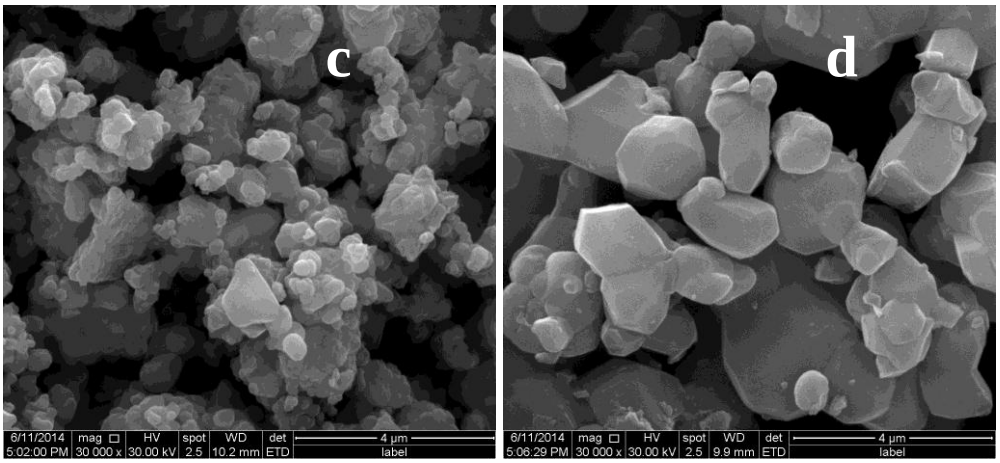

Figure 2. SEM images of the $LiCu_{0.04}Mn_{1.96}O_4$ materials prepared at different calcination temperatures (a) II500, (b) II600, (c) II700, (d) II800.

However, at the calcination temperature 800 ℃ for the grains had well-developed corners [20]. The particle size increase significantly with increasing two-stage calcination temperature from 500 ℃ to 800℃, which is quite in agreement with XRD results above. These results implying that the increase of calcination temperature can effectively promote the growth of grains, resulting in larger particle size.

3.3 Galvanostatic charge/discharge behavior

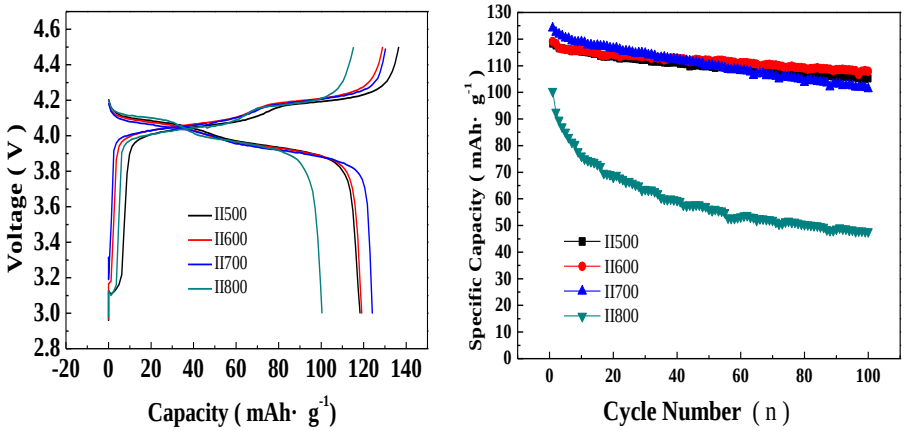

Figure 3. (a) The first charge and discharge curves at different calcination temperatures (a) II500, (b) II600, (c) II700, (d) II800 and the current densities of 0.5 C and (b) Cycle performances at current of 0.5 C.

Fig. 3(a) and (b) displays the initial galvanostatic charge and discharge profiles and cycling performance curves of $LiCu_{0.04}Mn_{1.96}O_4$ materials prepared by molten-salt combustion synthesis at 400 ℃ for 1h and two-stage calcination at 500 ℃, 600 ℃, 700 ℃ and 800 ℃ for 3 h. The cells cycled at 0.5 C in the voltage range of 3.0–4.5 V (vs. Li / Li^+). Fig. 3(a) shows the first charge and discharge

profiles of the samples at 0.5 C. All the samples display two obvious charge/discharge plateaus, corresponding to Li^+ insertion/extraction at two different tetragonal 8a sites in the spinel framework[6]. As can be seen from the Fig. 3 and Table 2, the $LiCu_{0.04}Mn_{1.96}O_4$ composites exhibit the initial discharge capacities were 118.3, 119.1, 124.1 and 100.4mAh g^{-1} at two-stage calcination for 500 ℃, 600 ℃, 700 ℃ and 800 ℃, respectively. The capacity retentions of the products after 100 cycles were about 88.9%, 90.6%, 81.6% and 47.5%, respectively. The initial discharge specific capacity of II700 was the highest, but the capacity retention was relatively lower. The initial discharge specific capacity of II600 was 119.1 mAh g^{-1}, Combined with our previous work, the initial discharge of $LiCu_{0.04}Mn_{1.96}O_4$ was as same as the $LiCu_{0.05}Mn_{1.96}O_4$ material [16], the discharge specific capacity of II600 was 107.9 mAh g^{-1} after 100 cycles, which was higher than those of the other samples. Therefore, the capacity rention of II600 product was optimal.

Table 2. Initial, 100th discharge capacities and capacity retention of all samples.

Cathode material	Discharge capacity (mAh/g)		Capacity retention (%)
	1st	100th	
II500	118.3	105.2	88.9
II600	119.1	107.9	90.6
II700	124.1	101.3	81.6
II800	100.4	47.7	47.5

3.4. Cyclic voltammetry

Fig 4 shows the cyclic voltammograms of $LiCu_{0.04}Mn_{1.96}O_4$ materials prepared by two-stage calcination at 500 ℃, 600 ℃, 700 ℃ and 800 ℃for 3 h. The cells cycled in the voltage range of 3.60–4.50 V (vs.Li/Li^+) and at a scan rate of 0.05 mV s^{-1}. Two pairs of similar redox peaks were observed in the CV curves for all materials, except for two-stage calcination at II500, which are can not well–developed at II500. Moreover, the peak intensity of 2nd and the 3rd in II800 rapidly decreases.

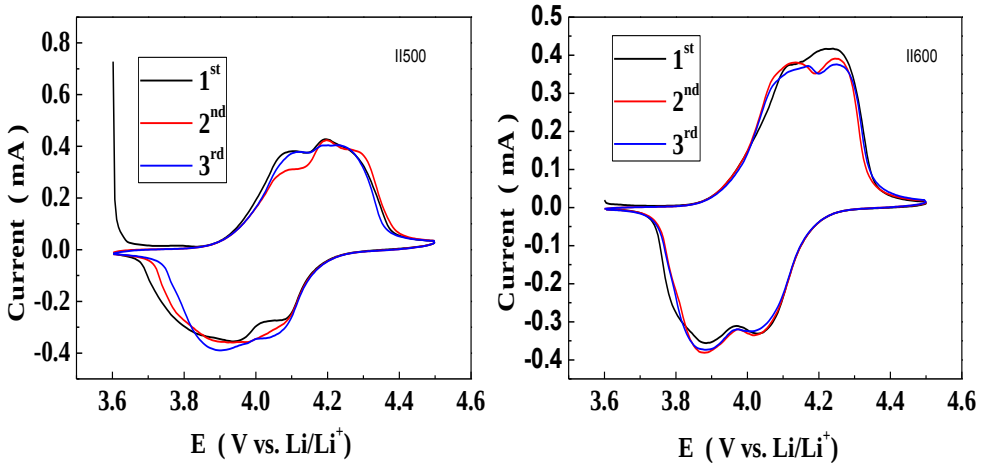

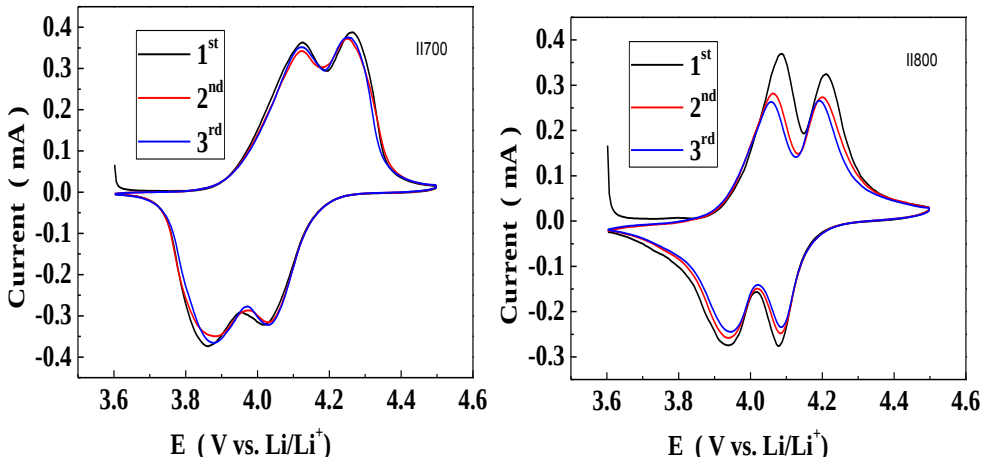

Figure 4. Typical CV curves of the 1st, 2nd, 3rd cycles for $LiCu_{0.04}Mn_{1.96}O_4$ electrode materials prepared by two-stage calcination at different temperatures with scan rate of 0.05 mV/s in the voltage range of 3.60–4.50 V.

The peak intensity at II600 and II700 slowly decreases, implying a better electrochemical performance. Consequently, This indicated that Cu-substitution had no severe effect on the redox potentials of $LiMn_2O_4$. Fig. 4 shows that the II600 sample exhibited higher peak current and peak area, indicating higher discharge specific capacity and electrochemical activity [21], which was consistent with the results from Fig.3(b).

4. CONCLUSIONS

The $LiCu_{0.04}Mn_{1.96}O_4$ materials were prepared by the molten-salt combustion method at different two-stage calcination temperatures. The II500, II600, II700 and II800 materials revealed initial discharge specific capacity of 118.3, 119.1 124.1 and 100.4 mAh g^{-1} and the capacity retention of 88.9%, 90.6%, 81.6% and 47.5% after 100 cycles at 0.5 C, respectively. It is believed that this synthetic method would be easily extended to large-scale production, which saves reaction time and energy at the same time. Consequently, The $LiMn_2O_4$ materials prepared by the molten-salt combustion method could be a competitive candidate cathode material for rechargeable lithium ion batteries.

ACKNOWLEDGEMENTS
This work was financially supported by the National Natural Science Foundation of China (51262031, 51462036), Program for Innovative Research Team (in Science and Technology) in University of Yunnan Province (2011UY09), Yunnan Provincial Innovation Team (2011HC008) and Innovation Program of Yunnan Minzu University (2015TX09, 2015YJCXZ24, 2015YJCXZ21).

Reference

1. H.Y. Zhao, F. Li, X.Q. Liu, C. Cheng, Z. Zhang, Y. Wu, W.Q. Xiong, B. Chen, *Electrochim. Acta*, 151 (2015) 263–269.

2. T. Shi, Y. Dong, C.M. Wang, F. Tao, L. Chen, *J. Power Sources*, 273 (2015) 959-965.
3. A.K. Mesfin, J.P. Maje, K. Niki, L.J. Roux, D. Mkhonto, I.O. Kenneth, K.M. Mkhulu, *Sustainable Energy Technologies and Assessments*, 5 (2014) 44-49.
4. D. Arumugam, G.P. Kalaignan, K. Vediappan, C.W. Lee , *Electrochim. Acta*, 55 (2010) 8439–8444.
5. X. Yi, X.Y Wang , B.W. Ju, Q.L.Wei, X.K. Yang, G.S. Zou, H.B. Shu, L. Hu, *J. Alloys Compd.*, 604 (2014) 50–56.
6. D. Arumugam, G.P. Kalaignan, *J. Electroanal. Chem*, 648 (2010) 54–59.
7. X. Gu, X.W. Li, L.Q. Xu, H.Y. Xu, J.Yang, Y.T. Qian, *Int. J. Electrochem. Sci.*, 7 **(**2012**)** 2504 – 2512.
8. R. Zeng, W. Li, D. Lv, Q. Huang, L. Zhao, *Trans. Nonferrous Met. Soc. China.*, 17 (2007) 1312-1318.
9. C.Y. Wang, S.G. Lu, S.R. Kan, J. Pang, W.R. Jin, X.J. Zhang, *J. Power Sources*, 189(2009) 607-610.
10. K.S. Lee, ST. Myung, H.J. Bang, S.J. Chung, Y.K. Sun, *Electrochim. Acta*, 52 (2007) 5201–5206.
11. F.X. Wang, S.Y. Xiao, Y. Shi, L.L. Liu, Y.S. Zhu, Y.P. Wu, J.Z. Wang and R. Holze, *Electrochim. Acta*, 93 (2013) 301-306.
12. L.F. Xiao, Y.Q. Zhao, Y.Y. Yang, Y.L. Cao, X.P. Ai, H.X. Yang, *Electrochim. Acta*, 54 (20 08) 545–550.
13. A.K. Mesfin, J.P. Maje, K. Niki, L.J. Roux, D. Mkhonto, K.I. Ozoemena, M.K. Mathe, *Sustainable Energy Technologies and Assessments*, 5 (2014) 44-49.
14. I. Taniguchi, N. Fukuda, M. Konarova, *Powder Technol.*, 181 (2008) 228–236.
15. J.J. Huang, F.L. Yang, Y.J. Guo, C.C. Peng, H.L. Bai, J.H.Peng, J.M. Guo, *Ceram. Int*, 41(2015)9662–9667.
16. J.J. Huang, Q.L. Li, H.L. Bai1, W.Q. Xu, Y.H. He, C.W. Su, J.H. Peng , J.M. Guo, *Int. J. Electrochem. Sci.*, 10 **(**2015**)** 4596 – 4603.
17. T.F. Yi, C.L. Hao, C.B. Yue, R.S. Zhu, *J. Shu, Synth. Met.*, 159 (2009) 1255–1260.
18. M.W. Xiang, L.Q. Ye, C.C. Peng, L. Zhong, H.L. Bai, C.W. Su, J.M. Guo, *Ceram. Int*, 40 (2014) 10839-10845.
19. C.H. Jiang, S.X. Dou, H.K. Liu, M. Ichihara, H.S. Zhou, *J. Power Sources*, 172 (2007) 410–415.
20. T. Nakamura , A. Kajiyama, *Solid State Ionics*, 124 (1999) 45–52.
21. L. He, S.C. Zhang, X. Wei, Z.J. Du, G.R. Liu, Y.L. Xing, *J. Power Sources*, 220 (2012) 228–235.